Examination for the Advancement to Candidacy

Thesis Research

# The Filter Diagonalization Method for the NMR data processing

Jianhan Chen

Department of Chemistry

University of California, Irvine

Examination Committee:

Professor David A. Brant, Chair

Professor Craig. C. Martens

Professor Benny R. Gerber

Professor Steven R. White

Professor Pierre F. Baldi, Dept. of Information and Computer Science

## ABSTRACT

Data processing in Nuclear Magnetic Resonance (NMR) is one of the bottlenecks in obtaining the spectral and eventually structural information about molecules. Conventional Fourier Transform (FT) spectral analysis has severe limitations, such as spectral resolution limited by FT uncertainty principle separately in each dimension; and typical high resolution methods are computationally expensive and numerically unstable. Recently, the Filter Diagonalization Method (FDM) has emerged as a new high resolution method for spectral analysis of multidimensional time signal. FDM solves the nonlinear Harmonic Inversion Problem (HIP) (i.e. fitting a time signal by $C(t) = \sum_k d_k e^{-it\omega_k}$ with unknowns $d_k \,\&\, \omega_k$) by pure linear algebra (diagonalizing some data matrices), and can potentially overcome all the said limitations. While the theory of FDM is already established, there are still many problems when applied to noisy signals. This report will address and solve some of these problems.

Although FDM is capable to extract accurately the parameters of narrow spectral peaks, in the presence of broad peaks (or strong background spectrum) and noise, the parameter list $\{\omega_k, d_k\}$ may contain some spurious (unphysical) entries. A new approach, the *multi-scale* FDM, is introduced to solve this problem, in which some coarse basis vectors describing (in low resolution) the global behavior of the spectrum are added to the narrow band Fourier basis. The *multi-scale* FDM is both stable and accurate, even when the total size of the basis used is much smaller than what would previously be considered as necessary for FDM. This, in turn, significantly reduces the computational cost.

In the multidimensional cases, the HIP is very ill-defined, e.g., the results are very sensitive to changes of the input data. Although better results can be obtained via averaging procedures which make use of this sensitivity, they are computationally expensive. A better way is to improve the structure of matrices prior to the diagonalization. Several regularization procedures are currently under investigation. Preliminary results are very encouraging. In addition, a high-resolution spectral estimator, the *Regularized Resolvent Transform* (RRT), which emerges naturally from FDM, is also introduced.

# 1. Introduction

NMR is one of the most powerful nondestructive techniques available today for probing the structure of matter. High-resolution NMR is valuable for determining the structure of chemical compounds; it is the only method capable of determining the 3-D structure of biomolecules in solution. However, while the sensitivity has been steadily improved with advances in NMR probe design, the fundamental resolution solely depends on the attainable magnetic fields and has seen only limited improvement over the same time. In pulsed NMR spectroscopy, time signals are first measured, then transformed to the frequency domain and analyzed. As such, data processing is a substantial part of the NMR spectroscopy and often the bottleneck to obtain the useful information.

Conventional pulsed NMR spectroscopy is known as Fourier Transform NMR because its sole dependence on FT to transform the time signals. Given a complex time signal $c_n(t) = c(n\tau)$, FT is defined as,

$$I(\omega) = i \int_0^\infty C(t)\, e^{i\omega t} dt \;\; \sim i\tau \sum_{n=0}^{\infty} c_n\, e^{in\tau\omega}, \tag{1}$$

where $\tau$ is the sampling time interval. FT is a linear method, which is considered fast, numerically stable and highly reliable. However, in the frame of FT, the spectral resolution in each frequency dimension is limited by the so called *FT time-frequency uncertainty principle*,

$$\delta F_l \sim \frac{1}{N_l \tau_l}\ , \tag{2}$$

where $N_l$ is the number of acquired time-domain points. Since each increment in an interferometric dimension requires at least one repetition of the entire pulse sequence, the time signal is almost always truncated in the indirect dimensions, especially in the case of high-dimensionality experiment, leading to poor resolution in these dimensions.

Due to this limitation as well as some others, extensive efforts have been devoted to the development of alternative techniques to FT. Most of these methods are based on some *a priori* knowledge about the signals. For example, in liquid state NMR experiments, usually all lines have Lorentzian lineshapes. In other words, the time signal can be modeled as a sum of damped sinusoids,

$$c(n) = \sum_k d_k \, e^{-in\tau\omega_k} = \sum_{k=1}^{K} d_k \, e^{-in2\pi\tau f_k} e^{-n\tau\gamma_k}. \tag{3}$$

If we can obtain the parametric representation of the signal, we know everything about the signal, and its infinite FT (Eq. 1) can be estimated. Inserting Eq. 3 into Eq. 1 and integrating analytically, we have,

$$I(\omega) \sim \sum_k \frac{d_k}{\omega_k - \omega} \, . \tag{4}$$

The problem of fitting the signals to Eq. 3 is known as *Harmonic Inversion Problem* (HIP). In principle, if the number of available signal points $N_{\max}$ dominates the number of unknowns $2K$, Eq. 3 can be solved exactly. Thus the resolution is not limited by the FT uncertainty principle (Eq. 2). It is only limited by the numerical accuracy of the HIP solver used. However, as HIP is a highly non-linear problem, in practical applications where the signals are noisy and contain thousands of peaks, it is numerically very difficult obtain an accurate and stable solution of Eq. 3. For example, in one of the well-known high resolution methods called Linear Prediction (LP), a parametric representation of the signal can be obtained (see ref. [1]). However, LP will generally fail for long and noisy signals, because large ill-conditioned non-linear problems have to be solved. This is true for most high resolution methods such as Maximum Entropy, Bayesian analysis etc [1]. Thus, FT remains the method of choice for most signal processing.

**The Theory of 1D FDM.**

Recently, the Filter Diagonalization Method (FDM) has emerged as a powerful high-resolution alternative to FT for processing time signals. It was originally designed by Neuhauser [2] for iterative diagonalization of large matrices which arise in quantum dynamics calculations when using a time-dependent approach. It was then reformulated and applied to spectral analysis of general experimental-measured time signals [3,4]. For the conventional evenly-spaced time signal, Mandelshtam and Taylor found a way to significantly improve its performance [4,5]. FDM has since found many applications in diverse fields and

in particular for processing NMR time signals [6–12,15]. In the rest of this introduction, the basic theory of 1D FDM will be first described, some existing problems then discussed. Multidimensional FDM will be discussed in the last section of this report.

There are two key assumptions in FDM. Firstly, the time signal can be modeled by Eq. 3, so that the spectral analysis problem can be turned into a Harmonic Inversion Problem. Secondly, the time signal can be associated with a time autocorrelation function of a fictitious dynamical system, which is described by an effective "Hamiltonian" operator $\hat{\Omega}$ that has complex eigenvalues $\{\omega_k\}$ [3],

$$c(n) = \left(\Phi_0 \middle| e^{-in\tau\hat{\Omega}}\Phi_0\right) \ . \tag{5}$$

Note that a complex symmetric inner product is used, $(a|b) = (b|a)$, without complex conjugation. $\Phi_0$ is some fictitious "initial state". Assume that there is a set of orthonormal eigenvectors, $\{\Upsilon_k\}$, that diagonalizes $\hat{\Omega}$, we can write,

$$\hat{\Omega} = \sum_k \omega_k |\Upsilon_k)(\Upsilon_k| \ . \tag{6}$$

where the eigenvectors are orthonormalized with respect to the complex symmetric inner product, i.e.,

$$(\Upsilon_k|\Upsilon_{k'}) = \delta_{kk'} \ . \tag{7}$$

Inserting Eq. 6 into Eq. 5, we obtain Eq. 3 with

$$d_k^{1/2} = (\Upsilon_k|\Phi_0) \ . \tag{8}$$

Therefore the harmonic inversion problem of Eq. 3 becomes equivalent to diagonalizing the "Hamiltonian" $\hat{\Omega}$ or, equivalently, the evolution operator $\hat{U} \equiv e^{-i\tau\hat{\Omega}}$:

$$\hat{U}\Upsilon_k = u_k\Upsilon_k \ , \tag{9}$$

with $u_k = e^{-i\tau\omega_k}$. The *eigenvalues* of $\hat{U}$ thus determine $\{\omega_k\}$, *line positions* and *widths*, and the *eigenvectors* determines $\{d_k\}$, *line amplitudes* and *phases*. While the fitting problem of Eq. 3 is highly non-linear, the eigenvalue problem (Eq. 9) to be solved in FDM is linear. This guarantees uniqueness of the solution and intrinsic stability of FDM.

Even though neither $\hat{U}$ or $\Phi_0$ is explicitly available, the matrix representation of $\hat{U}$ in an appropriately chosen basis set $\{\Psi_j\}$ can be computed purely from the time signal $c(n)$. Moreover and more importantly, when a narrow band Fourier-type basis is chosen, the resulting matrix is diagonally dominant with decaying off-diagonal elements. This implies that the diagonalization of $\hat{U}$ can be carried out in a block-diagonal fashion by simply ignoring all the elements outside a given block. In other words, instead of analyzing the whole spectrum at one time, we can divide it into small spectral windows and analyze them separately. A rectangular Fourier basis [4] reads

$$\Psi_j = \sum_{n=0}^{M_{\max}} e^{in\tau\varphi_j}\Phi_n \ , \tag{10}$$

with the Krylov vectors defined as

$$\Phi_n \equiv \hat{U}^n\Phi_0 = e^{-in\tau\hat{\Omega}}\Phi_0 \ , \tag{11}$$

and $\{\varphi_j\}$ being a set of $K_{\rm win}$ equidistant values taken inside a small frequency window of interest. Assuming that the eigenvectors can be expanded in the Fourier basis,

$$\Upsilon_k = \sum_j \left[\mathbf{B}_k\right]_j \Psi_j \ , \tag{12}$$

the operator eigenvalue problem, Eq. 9, is then cast into a generalized matrix eigenvalue problem (GEP),

$$\mathbf{U}^{(1)}\mathbf{B}_k = u_k\mathbf{U}^{(0)}\mathbf{B}_k \ , \tag{13}$$

where $U^{(p)}$ is the matrix representation of $\hat{U}^p$. The matrix elements can be evaluated as,

$$\begin{aligned}\left[\mathbf{U}^{(p)}\right]_{jj'} &= \left(\Psi_j|\hat{U}^p\Psi_{j'}\right) \\ &= \hat{S}\sum_{\sigma=0,1}\frac{e^{i\sigma[\tau M(\varphi_{j'}-\varphi_j)+\pi]}}{1-e^{i\tau(\varphi_{j'}-\varphi_j)}}\sum_{n=\sigma M}^{(\sigma+1)(M-1)} e^{in\tau\varphi_j}c(n+p)\end{aligned} \tag{14}$$

where $\hat{S}$ defines symmetrization operator over the indices $j$ and $j'$:

$$\hat{S}\ g_{jj'} = g_{jj'} + g_{j'j} \ . \tag{15}$$

Eq. 14 is, in principle, correct for all choices of $\varphi$ and $\varphi_{j'}$ except for the singularity arising at $\varphi_j = \varphi_{j'}$. To obtain a numerically practical expression for this singular case we evaluate the $\varphi_j \to \varphi_{j'}$ limit leading to

$$\left[\tilde{\mathbf{U}}^{(p)}\right]_{jj} = \sum_{n=0}^{2M-2} e^{in\tau\varphi_j}(M - |M-n-1|)c(n+p) \ . \tag{16}$$

Solving Eq. 13, the eigenvalues $u_k = e^{-i\tau\omega_k}$ then yield the frequencies $\omega_k$ and the eigenvectors $\mathbf{B}_k$, the amplitudes,

$$d_k^{1/2} = \sum_j [\mathbf{B}_k]_j \, (\Psi_j|\Phi_0) = \sum_{j=1}^{K_{\rm win}} \left[\tilde{\mathbf{B}}_k\right]_j \sum_{n=0}^{M-1} e^{in\varphi_j} c(n) \ . \tag{17}$$

which follows from Eqs. 8, 10 and 12.

Therefore, given a complex time signal, we can first pick up a spectral window of interest (which is usually much smaller than Nyquist Range), evaluate the $U^{(p)}$ matrices using Eqs. 14 and 16, insert them into Eq. 13 and solve the GEP using any standard eigenvalue problem solvers, calculate $\{\omega_k\}$ from eigenvalues and $\{d_k\}$ from eigenvectors using Eq. 17, and then obtain a parameter classification of the time signal. Once the parameter list $\{\omega_k, d_k\}$ is available, different spectral representations can be constructed. While in FDM there is a lot of freedom to play with the line list and construct different *ersatz* spectra, Eq. 4 is consistent with infinite FT and most used. Usually an absorption mode spectrum is preferred, which is obtained by taking the imaginary part of the correctly phased complex spectrum $I(\omega)$,

$$A(\omega) \sim \sum_{k=1}^{K} \mathrm{Im}\left\{\frac{d_k}{\omega_k - \omega}\right\} \ , \tag{18}$$

**Performance and Existing Problems**: Tested with model and experimental signals, FDM has shown great promise in both cases. For signals with relatively high signal to noise ratio (SNR), FDM is able to provide well converged spectra using signals much shorter than what would be necessary for FT. In addition FDM can provide a high fidelity line list, given that the signal can be well modeled by Eq. 3 and the $U$ matrices in Fourier basis are block diagonalizable. Examples can be found in Refs. [6–12,15].

However, tested later with more noisy signals, FDM started to show various problems. It was found that for signals with low SNR or with some significant background (e.g., very

broad peaks, big baseline rolls etc.), FDM would show some instability. Unphysical poles which have positive Im$[\omega_k]$ & big $d_k$ will show up in the line list as well as other types of "spurious" entries. Spectra constructed using direct formula Eq. 4 will then show baseline distorted in some regions and are sensitive to the FDM parameters used. One example is given in Fig.1, corresponding to a very noisy NMR signal for progesterone [7] with many overlapping peaks. Qualitatively, this instability can be due to the narrow band Fourier basis (Eq. 10) used. The latter is highly localized in the frequency domain. While this is a big advantage of the Fourier basis which leads to the block diagonalizability of U matrices, in the presence of noise, each narrow band basis function $\Psi_j$ is "locked" on the noise peaks that appear close to $\varphi_j$ (see Eq. 10) and cannot "see" the peaks that are far away. Thus a narrow band basis will be inadequate to represent a broad spectral feature that is not localized in a single window. This may cause ambiguity in reproducing the broad spectral features or the baseline, and is the source of instability. Such instability can sometimes be reduced by using larger windows. However, increasing the basis size does not always work, and even when it does, it is impractical due to very unfavorable scaling of the computational cost for an eigenvalue solver. Several hybrid spectral construction methods, which combine FT and FDM, can also be applied to correct the *ersatz* spectra [13], but then we do not have a line list which is consistent with the spectrum provided. Our goal here is to find a numerical efficient method which can provide us a well converged *ersatz* spectrum as well as a consistent line list.

## 2. Multi-Scale Fourier Basis

As mentioned above, the instability in the FDM line list may occur because localized basis functions do not describe correctly the spectral peaks that are broader than the width of the spectral window. To take into account the global features but avoid the use of a big Fourier basis we need to add to our narrow band and dense window basis some sparse *coarse* (i.e., delocalized) basis functions. Since the broad peaks do not require high resolution we will need only a few such coarse basis functions. We also want to minimize the number of

coarse basis functions with the condition that the non-localized features that may affect the local spectral analysis are represented adequately.

Given that the farther away from the current window, the less significant the effect of a broad spectral feature to the local analysis, the coarse basis could be chosen such that the spacing between the adjacent coarse basis functions and, accordingly, their bandwidth, monotonically increase with respect to the distance between the center of the basis function ($\varphi_j$) and the spectral window of interest. Thus only the features, which are broad enough to affect the current window, will be captured by the coarse basis. Here the local density of the basis functions is defined as

$$\rho_j = \frac{2\Delta\varphi_{\min}}{|\varphi_{j+1} - \varphi_{j-1}|} \tag{19}$$

where $\Delta\varphi_{\min} = 2\pi/\tau M_{\max}$ is determined by the spacing between the narrow band Fourier basis functions. The Fourier length should be scaled accordingly to the local density using $M_j = \rho_j M_{\max}$, which makes the bandwidth of the basis functions consistent with the basis density. For a given small spectral window we can construct a multi-scale basis, which contains $K_{\text{win}}$ narrow band Fourier basis functions localized in the window and $K_{\text{c}}$ coarse basis functions spread over a wide spectral range:

$$|\Psi_j) = \sum_{n=0}^{M_j-1} e^{in\varphi_j} |\Phi_n), \quad j = 1, 2, \ldots, K = K_{\text{win}} + K_{\text{c}} \tag{20}$$

with the Fourier length $M_j$ depending on $j$: $M_j = M_{\max}$ for the narrow band, and $M_j = M_{\max}\ \rho_j$, for the coarse basis functions.

The $\mathbf{U}$ matrix representations can also be efficiently evaluated in terms of the time signal. For the off diagonal matrix elements, i.e., when $\varphi_j \neq \varphi'_j$, we have,

$$\begin{aligned}\left[\mathbf{U}^{(p)}\right]_{jj'} &= \hat{S} \sum_{\sigma=0,1} \frac{e^{i\sigma[(M_{j'}+1)\tau(\varphi_{j'}-\varphi_j)+\pi]}}{1 - e^{i\tau(\varphi_{j'}-\varphi_j)}} \\ &\times \sum_{n=\sigma(M_{j'}+1)}^{\sigma M_{j'}+M_j} e^{in\tau\varphi_j} c(n+p) \ ,\end{aligned} \tag{21}$$

For the diagonal matrix elements, $\varphi_j = \varphi_{j'}$, the expression is equivalent to that previously derived [4]:

$$\left[\mathbf{U}^{(p)}\right]_{jj} = \sum_{n=0}^{2M_j} (M_j + 1 - |M_j - n|) e^{in\tau\varphi_j} c(n+p) \ . \tag{22}$$

Once the U-matrices are available one can solve the generalized eigenvalue problem Eq. 13 to obtain the eigenvalues $u_k$ and eigenvectors $\mathbf{B}_k$. Due to Eqs. 17 and 20 the latter yield the amplitudes using

$$\sqrt{d_k} = \sum_{j=1}^{K} [\mathbf{B}_k]_j \sum_{n=0}^{M_j} e^{in\tau\varphi_j} c(n) \tag{23}$$

Fig. 2 shows an example of such a basis set for a particular window together with the FDM ersatz spectrum obtained using this basis and plotted, intentionally, in a wide spectral range. As expected, fine features are captured inside the window where dense and narrow band basis functions are used, and only coarsely resolved features appear in the region outside this window. Furthermore, the spectral resolution decreases smoothly in the directions away from the window, so there are no edge effects associated with the local spectral analysis. This makes it easy to combine the results of different windows to construct the overall spectrum. Looking into the line lists reveals that with multi-scale Fourier basis the line list contains much fewer "spurious" poles. Unphysical poles with positive $\mathrm{Im}[\omega_k]$ & big $d_k$ basically do not occur. So that we do not need any hybrid method to estimate the spectrum, and can simply use Eq. 4. In addition, the availability of more accurate parameters facilitates investigation of more sophisticated methods to obtain some reduced line list.

**Double-Scale Fourier basis**: Unlike the example shown in Fig. 2 which might seem to be a little complicated, for the simplest realization of a multi-scale Fourier basis one can consider just two scales with $M_j = M_{\max}$, for the narrow band window basis, and $M_j = M_c \ll M_{\max}$, for the coarse basis, corresponding to having two equidistant grids with spacings, $\Delta\varphi_{\min} = 2\pi/\tau(M_{\max}+1)$ and $\Delta\varphi_c = 2\pi/\tau(M_c+1)$, respectively. This simplifies the calculation of the U-matrix elements. Furthermore, the coarse basis can be reduced (or contracted) by keeping only those basis functions $\Psi_j$ for which no significant peaks appear in a low resolution Fourier spectrum around $\varphi_j$. The next two examples given below are obtained with double-scale implementation.

Fig. 3 shows some spectra obtained with the double-scale basis. The use of a coarse

basis does improve the appearance of the spectrum significantly, even when very few basis vectors are used. Furthermore, due to the removal of the edge effects by the latter, the size of the narrow band basis could be very small as well, compared to the previous single-scale version of FDM. As such, for the example considered here about $K_c = 7$ coarse basis functions, retained after the contraction procedure, and $K_{\rm win} \geq 10$ window basis functions were needed to obtain well converged ersatz spectra.

Fig. 4 presents an IR spectrum. The interferogram contained 4744 data points that were processed by both FT and multi-scale FDM to generate the absolute value spectra $|I(\omega)|$. The FT spectrum is very hard to interpret and, probably, hard to quantify by conventional means as the peaks are not quite narrow and both the overlapping effects and the interference with the background are significant. Unlike the FT case, the FDM peaks are generally much sharper. Notably and most importantly, the FDM spectrum is fit by the form of Eq. 3, so the parameters of the peaks (such as the positions, widths and amplitudes) are known. At the same time, fitting $|I(\omega)|$ by Lorentzians would be a very challenging project. We also point out that the overall shape of the spectrum is reproduced well by the multi-scale FDM, while the single-scale version is very unstable for this signal because of the very big background.

**Extension to multidimensional cases**: Armed with Eqs. 20, 21 and 23, multi-scale Fourier basis can be extended to multidimensional FDM (Multi-D FDM). Details can be found in Ref. [13]. At this point, there are some totally different problems in multidimensional FDM which need to be solved first. It is hard to determine how multidimensional multi-scale Fourier basis behaviours before these problems are solved. The existing problems in Multi-D FDM will be addressed in the next section.

## 3. Multidimensional FDM

The 1D formalism given in the introduction can be extended to process multidimensional time signals. We will use the 2D case as example. Further extension to a more than 2D case is straightforward and the corresponding expressions are analogous. We will first briefly

review the 2D FDM theory, then discuss the existing problems and describe several attempts to solve the problems. Detailed Multi-D FDM theories can be found in Refs. [4,5,14].

Given a complex 2D time signal $c(\vec{n}) \equiv C(n_1\tau_1, n_2\tau_2)$, where $\vec{n}$ is the time vector, defined on a rectangular equidistant time grid of size, we need to find a parametric fit of the whole data set to the following model,

$$c_{\vec{n}} = \sum_k d_k e^{-i\vec{n}\vec{\omega}_k} \equiv \sum_k d_k \prod_{l=1}^{2} e^{-in_l\tau_l\omega_{lk}} \ , \tag{24}$$

where $\vec{\omega}_k \equiv (\omega_{1k}, \omega_{2k})$ are vectors of unknown complex frequencies, $\omega_{lk} = \nu_{lk} - i\gamma_{lk}$, and $d_k$, unknown complex amplitudes. This is a 2D *harmonic inversion problem* (2D HIP). Just like 1D HIP, it can be cast into a family of generalized eigenvalue problems, by associating the 2D time signal to a double-time correlation function of a fictitious quantum system with two commuting non-Hermitian symmetric Hamiltonians $\hat{\Omega}_1$ and $\hat{\Omega}_2$ [5,10,12,14],

$$c(\vec{n}) = \left(\Phi_0 \middle| e^{-i\vec{n}\vec{\Omega}}\Phi_0\right) \equiv \left(\Phi_0 \middle| e^{-in_1\tau_1\hat{\Omega}_1 - in_2\tau_2\hat{\Omega}_2}\Phi_0\right) \ . \tag{25}$$

The Hamiltonians are assumed to have spectral representations,

$$\hat{\Omega}_l \Upsilon_{lk} = \omega_{lk}\Upsilon_{lk} \ , \quad l = 1, 2 \ . \tag{26}$$

Inserting Eq. 26 into Eq. 25, we can obtain

$$c(\vec{n}) = \sum_{k_1,k_2} d_{k_1k_2} e^{-in_1\tau_1\omega_{1k_1} - in_2\tau_2\omega_{2k_2}} \tag{27}$$

with

$$d_{k_1k_2} = T_{k_1k_2} b_{1k_1} b_{2k_2} \equiv (\Upsilon_{1k_1}|\Upsilon_{2k_2})(\Phi_0|\Upsilon_{1k_1})(\Phi_0|\Upsilon_{2k_2}) \tag{28}$$

A 2D spectral representation that corresponds to a 2D Fourier integral of the signal can then be written in terms of the Green's functions (or resolvent operators),

$$I(\omega_1, \omega_2) = \left(\Phi_0 \middle| \ \hat{G}_1(\omega_1)\ \hat{G}_2(\omega_2)\ \Phi_0\right) = \sum_{k_1,k_2} \frac{d_{k_1k_2}}{(\omega_{1k} - \omega_1)(\omega_{2k} - \omega_2)} \ , \tag{29}$$

where an $l$-th Green's function can be represented in terms of the $l$-th eigenvectors and eigenvalues,

$$\hat{G}_l(\omega_l) \equiv \frac{1}{\hat{\Omega}_l - \omega_l} \equiv \sum_k \frac{|\Upsilon_{lk})(\Upsilon_{lk}|}{\omega_{lk} - \omega_l} \ . \tag{30}$$

Note that although we assume that the Hamiltonians $\hat{\Omega}_1$ and $\hat{\Omega}_2$ commute with each other, Eq. 26 does not assume that $\Upsilon_{1k} = \Upsilon_{2k}$, or equivalently, that $(\Upsilon_{1k}|\Upsilon_{2k'}) = \delta_{1k,2k'}$. The purpose is to avoid the problem of finding a unique set of eigenvectors which simultaneously diagonalizes both Hamiltonians, because in cases of noisy signal or signal with degenerated poles such a unique set of eigenvectors does not necessarily exist. In other words, $T_{k_1k_2} = (\Upsilon_{1k_1}|\Upsilon_{2k_2})$ is not necessarily diagonal; nor can it necessarily be reduced to diagonal form by permutations. However, if we let $(\Upsilon_{1k}|\Upsilon_{2k'}) = \delta_{1k,2k'}$ in Eq. 28, the representation Eq. 27 boils down to the ideal representation of Eq. 24. Thus adopting representation of Eq. 27 covers the case of degenerate spectra and avoids the necessity of generating a unique set of eigenvectors $\{\Upsilon_k\}$, making the 2D FDM more robust and applicable to noisy time signals.

Matrix representations of the associated evolution operators $\hat{U}_l = e^{-i\tau_l n_l \hat{\Omega}_l}$ are also available in terms of 2D time signals. Similarly to 1D case, a 2D Fourier-type basis is used and resulting $U$ matrices can be block diagonalized (see Refs. [12,14,22] for more details of computing $\tilde{U}^{(p)}$ matrices). The operator eigenvalue problems in Eq. 26 can be then cast into two generalized eigenvalue problems (GEP),

$$\tilde{\mathbf{U}}_l \tilde{\mathbf{B}}_{lk} = u_{lk} \tilde{\mathbf{U}}_0 \tilde{\mathbf{B}}_{lk} \ , \quad l = 1, 2 \ . \tag{31}$$

Solving these two GEPs, we can obtain $\{\omega_{lk}\}$ and $\{d_{k_1k_2}\}$ from the eigenvalues and eigenvectors (also see Refs. [12,14,22]).

**Performance and Problems**: Unfortunately, the formalism given above works well only for model signals and signals with extremely high SNR. Single FDM calculation was never free of artifacts for most realistic signals. One example is show in Fig. 5(a), where applied to a HSQC NMR 2D signal. The spectrum shows some high resolution characters but is contaminated by various artifacts, such as spurious spikes randomly distributed over the frequency domain and poorly converged genuine peaks. Moreover, this artifact pattern is very sensitive to both the small variations in the input data and the parameters of the FDM calculation. At this point it is still not absolutely clear what exactly causes instability in

the 2D FDM. However, one can make use of this high sensitivity and apply some averaging to reduce the artifacts. Two averaging procedures, *signal length averaging* and *pseudo-noise averaging*, were used [11,14,22]. However, averaging methods are very time consuming and can not provide any meaningful line list.

Careful studies of the U matrices show that they are generally ill-conditioned in multi-dimensional cases. Applying of SVD to the U matrices shows that the condition number* of the U matrices is often very large (e.g., can go up to $10^{12}$ sometimes). This means that the matrices are very singular and the basis is over-completed. Partially, this can be justified by considering the direct product type basis used. In multi-D FDM, the size of 2D FT basis scales as one forth of the total number of data points used, i.e., $N_{\rm basis} \sim N_{\rm 1max}/2 \times N_{\rm 2max}/2$, while the number of peaks present is usually much smaller even for spectra which contain many direct product pattern clusters of peaks such as TOCSY spectra. Therefore, we need find some way to improve the matrix structure before diagonalization. There are a few potential ways now under investigation.

## 4. Regularization of FDM

**Reducing the basis size using SVD**:

Singular Value Decomposition (SVD) is very reliable, well developed method which can analyze the null and range space of a given matrix. For a square $N \times N$ matrix $\mathbf{R}$, SVD can decompose it as,

$$\mathbf{R} = \mathbf{W}\mathbf{\Lambda}\mathbf{V}^{\dagger}, \tag{32}$$

where $\mathbf{W}$ and $\mathbf{V}$ are unitary $N \times N$ matrices, and $\mathbf{\Lambda} = \mathrm{diag}(\lambda_i)$, a real diagonal matrix with singular values with $\lambda_1 \geq \lambda_2 \geq ... \geq \lambda_N \geq 0$. The columns of matrix $\mathbf{W}$( or equivalently, those of matrix $\mathbf{V}$) form an orthonormal set of basis vectors which covers both the nullspace

*Condition number is defined as the ratio of maximum singular value to the minimum singular value of the matrix. The bigger is the condition number, the more singular is the matrix.

(if any) and range of matrix $\mathbf{R}$. Specifically, the columns of $\mathbf{W}$, whose same-numbered elements $\lambda_i$ are *nonzero*, form an orthonormal set of basis vectors that span the range; the columns of $\mathbf{V}$, whose same-numbered elements $\lambda_i$ are *zero*, form an orthonormal basis for the nullspace [17]. Thus, by checking the singular values, one would be able to analyze how ill-conditioned the matrix is and find out the range and null space. Once the range space identified, one can then re-evaluate $\mathbf{R}$ in the corresponding basis set and obtain a new matrix $\tilde{\mathbf{R}}$, which is much better behaviored.

For real signal with noise, there will be only 'big' and ' small' singular values. One then hopes for situations where $\{\lambda_i\}$ shows some abrupt magnitude change, so that by setting a suitable cutoff one can get rid of the nullspace. This may be true in some cases, such as when the corresponding spectra contain relatively separated peaks and are not too contaminated by noise. Fig. 5 shows four 2D $^{15}\mathrm{N} - {}^{1}\mathrm{H}$ shift correlation spectra obtained from a sample of nitrogen-15 labeled rubredoxin, a small metalloprotein [18]. Only 16 increments are used in the $^{15}$N dimension, with 200 complex points along the $^{1}$H dimension. The initial basis size is then $50 \times 8 = 400$. Plottings of singular values (top panel) clearly show an abrupt magnitude change at around $i \sim 30$. Setting a cutoff at this point will give a very clean, well converged spectrum (panel c in Fig. 5). We do not actually need to throw away so many basis vectors. Panel b in Fig. 5 shows that even throwing away only 23 basis vectors corresponding to the smallest 23 singular values already reduces most of the artifacts. Further reduction of the basis size to around 150 will basically yield the same spectrum as shown in panel c (not shown). While it is safe to keep a little more basis vectors, it is extremely dangerous to throw away more than necessary, which could lead to missing genuine peaks(e.g., panel d. in Fig. 5). This is a big disadvantage of such an aggressive procedure. Even worse, typical NMR data may not have such a clean break in singular values. Then choosing any cutoff can be very risky, giving the operator a tremendous chance to bias the experimental results to support some particular viewpoint. Therefore, such a procedure is not generally applicable. Better procedures should be more conservative, applying "soft cutoff" instead of the "hard cutoff".

**Soft Regularizations**

Regularization is the center aspect when dealing with ill-conditioned systems. Reducing the basis size using truncated SVD can be considered as a simple regularization. A more consistent and systematic regularization can be implemented in the framework of resolvent expressions for spectral estimation, which are derived below.

The assumption of Eq. 5 can be rewritten using the evolution operator, $\hat{U} \equiv e^{-i\tau\hat{\Omega}}$,

$$c(n\tau) = \left(\Phi_0 | \hat{U}^n \Phi_0\right) \ , \tag{33}$$

Substitute Eq. 33 into Eq. 1 and evaluate the geometric sum analytically, we obtain

$$I^\tau(\omega) = \left(\Phi_0 \middle| \hat{G}^\tau(\omega)\, \Phi_0\right) = \left(\Phi_0 \middle| \frac{i\tau}{1 - e^{i\tau\omega}\hat{U}}\, \Phi_0\right) \ . \tag{34}$$

Evaluate this operator function in the Fourier basis yields the resolvent formula,

$$I^\tau(\omega) \approx i\tau\ \mathbf{C}^{\mathrm{T}} \mathbf{R}(\omega)^{-1} \mathbf{C} \ , \tag{35}$$

with $\mathbf{R}(\omega) = \mathbf{U}_0 - e^{i\tau\omega}\mathbf{U}_1$ and $\mathbf{C}$ the Fourier transform of time signal vector $\mathbf{C} = \{c(n\tau)\}$,

$$[\mathbf{C}]_j = \sum_{n=0}^{M-1} e^{in\tau\varphi_j}\, c(n\tau) \ , \tag{36}$$

These expressions are for 1D case, and can be easily rewritten for multi-D cases. Details can be found in Refs. [19,22]. Expressions for 2D case are as follows,

$$I^\tau(\omega_1, \omega_2) \approx -\tau_1\tau_2\ \mathbf{C}^{\mathrm{T}} \left\{\mathbf{R}_1(\omega_1)^{-1} \mathbf{U}_0 \mathbf{R}_2(\omega_2)^{-1}\right\} \mathbf{C} \tag{37}$$

with

$$\mathbf{R}_l(\omega_l) = \mathbf{U}_0 - e^{i\tau_l\omega_l}\mathbf{U}_l \ , \quad l = 1, 2 \ , \tag{38}$$

$$[\mathbf{C}]_j = \sum_{n_1=0}^{M_1-1} \sum_{n_2=0}^{M_2-1} e^{in_1\tau_1\varphi_{1j}} e^{in_2\tau_2\varphi_{2j}}\, c(n_1\tau_1, n_2\tau_2) \ . \tag{39}$$

Then it becomes clear that any singularities in matrix $\mathbf{R}_l(\omega_l)$ will result in artifacts in $I(\omega_1, \omega_2)$, and it is $\mathbf{R}_l(\omega_l)$ that need to be regularized.

**Regularized Resolvent Transform (RRT)**: One way to evaluate the resolvent formula, Eq. 35 and Eq. 37, is solve the corresponding GEPs, Eq. 13 (1D) or Eq. 31 (2D), to obtain the parameters and then use Eq. 4 or Eq. 29. This is the approach used in FDM. Alternatively, as both $\mathbf{C}$ and $\mathbf{R}$ are available, Eq. 35 and Eq. 37 can be used to estimate the infinite time DFT directly without solving the GEPs.

In order to regularize Eq. 35 or Eq. 37 one can replace the true inverse $\mathbf{R}^{-1}$ by a pseudo-inverse $\mathbf{R}_q^{-1}$ with some regularization parameter $q$, arriving at the *Regularized Resolvent Transform* (RRT) [19],

$$I^{\tau}(\omega) = \mathbf{C}^{\mathrm{T}}\mathbf{R}_q^{-1}\mathbf{C} \ . \tag{40}$$

Now there are several options. One possibility is to use SVD of $\mathbf{R}(\omega)$ to calculate a pseudo-inverse by discarding the singular subspace. However, SVD, if applied for each value of $\omega$, would be quite computationally expensive. A much less expensive regularization of the resolvent can be obtained using the Tikhonov Regularization [21] in which a pseudo-inverse is obtained according to

$$\mathbf{R}_q^{-1} = \left(\mathbf{R}^{\dagger}\mathbf{R} + q^2\right)^{-1}\mathbf{R}^{\dagger} \ , \tag{41}$$

where dagger means Hermitian conjugate, and $q$ is a real number. With such a regularization the singularity in the denominator is removed as $\left(\mathbf{R}^{\dagger}\mathbf{R} + q^2\right)$ is a Hermitian and positive definite matrix. Eq. 35 and Eq. 37 can then be evaluated by solving the regularized Hermitian least squares problem,

$$\left(\mathbf{R}_l^{\dagger}(\omega_l)\tilde{\mathbf{R}}_l(\omega_l) + q^2\right)\tilde{\mathbf{X}}_l(\omega_l) = \tilde{\mathbf{R}}_l^{\dagger}\tilde{\mathbf{C}} \, , \quad l = 1, 2 \, , \tag{42}$$

and then using

$$I^{\tau}(\omega) = i\tau \ \mathbf{C}^{\mathrm{T}}\mathbf{X}(\omega) \, , \tag{43}$$

$$I^{\tau}(\omega_1, \omega_2) = -\tau_1\tau_2 \ \mathbf{X}_1(\omega_1)^{\mathrm{T}}\mathbf{U}_0\mathbf{X}_2(\omega_2) \, . \tag{44}$$

In RRT only complex spectra will available. Absorption mode spectrum can be obtained by taking the imaginary part of the correct phased complex spectrum in 1D case; in 2D case,

double absorption can be obtained from a pair of amplitude modulated signals or from a pair of N- and P-type data sets by taking appropriate linear combinations.

RRT corresponds to a direct nonlinear transformation of the time signal to the frequency domain. Unlike most other nonlinear spectral estimators, RRT is very stable with the regularization parameter $q$ controlling both the stability and resolution, whether used in SVD or Tikhonov Regularization: a bigger $q$ suppresses the spectral artifacts, decreases the resolution, and therefore leads to more uniform spectral estimate. 1D examples can be found in Ref. [19]. In the next example, we apply 2D RRT to a frequently-employed 2D experiment to correlate proton and nitrogen-15 chemical shifts. The 2D shift correlation spectra of the nitrogen-15 labeled metalloprotein rubredoxin [18] shown in Fig. 6 are particularly favorable for FFT analysis because a phase-sensitive spectrum can be computed and the peaks are of similar intensity, so that a poorly-resolved intense peak does not mask a weaker feature nearby. Nevertheless, RRT yields a welcome improvement in resolution, or a decrease in the experiment time for a similar resolution. As in FDM, the gain in resolution hinges on the spectrum having sufficient signal-to-noise ratio. It is neither possible to improve the resolution of noisy spectra, nor to magically divine the presence of peaks buried in noise.

Just like DFT, the RRT, while being amazingly stable and easy to use, has some drawbacks: (i) it is a spectral estimator and as such does not automatically provide one with a line list; (ii) generally, one has difficulties in constructing absorption mode spectra in multidimensional spectral estimation when a single purely phase modulated data is processed, while in FDM various types of spectra are easily constructed using the computed spectral parameters; (iii) it is not obvious how to construct an absorption mode J-spectrum with RRT.

**FDM2K**: A rather more attractive, than the truncated SVD, seems to be the procedure, reminiscent to the Tikhonov regularization, in which Eq. 31 for each $l = 1, ..., \mathrm{D}$ is modified as [20]

$$\mathbf{U}_0^\dagger \mathbf{U}_l \mathbf{B}_{lk} = u_{lk} \left( \mathbf{U}_0^\dagger \mathbf{U}_0 + q^2 \right) \mathbf{B}_{lk} \ , \tag{45}$$

with regularization parameter q. The new generalized eigenvalue equations have a Hermi-

tian and positive definite right hand side matrix, which may be advantageous for numerical solution. It is very tempting to treat $q$ as the "noise power", just like in the Maximum Entropy applications [1]. Indeed, it can be demonstrated semiquantitatively [20], that the spectral features with amplitudes $d_k$ of order of $q$ and below are smoothed out, while the stronger peaks remain essentially unaffected. However, how the spectra are distorted (regularized) by $q$ is still not fully understood. Quite surprisingly, the results of using Eq. 45 for some 2D [20] applications are very encouraging, although the element of ambiguity in the choice of $q$ is still the main issue. It is, therefore, recommended to generate a family of spectra as a function of $q$, treating the latter as a parameter of the method, just like the form of apodization function in DFT.

There are a few points need to be pointed out. First, compared to the Tikhonov Regularization in RRT, the regularization in FDM2K is not a consistent regularization. It is a "good" regularization only when matrices $\mathbf{U}_1$ and $\mathbf{U}_2$ are "bigger" than $\mathbf{U}_0$. This is usually true as signals shall decay in the time domain. However, in case of noisy signals, some components of $\mathbf{U}_1$ or $\mathbf{U}_2$ may be smaller than corresponding counterparts of $\mathbf{U}_0$, and will introduce new artifacts. Second, Eq. 45 is not symmetric any more when $q \neq 0$. Thus to solve Eq. 45 exactly, one need to calculate both left and right eigenvectors (for symmetric left and right matrices, the left and right eigenvectors are the same). It is usually accurate enough to just calculate the right eigenvectors, when $q$ is small compared to the norm of the matrices and the eigenvectors are used only for calculating the amplitudes $\{d_k\}$. However, in other cases such as J spectra, one need to use the eigenvectors to construct the projection operators. Then both left and right eigenvectors must be calculated [23].

The regularization corresponding to the use of Eq. 45 has been tested for some 2D HSQC spectra always showing good results and had been named *FDM2K* [20] to the honor of new Millennium. FDM2K is demonstrated in Fig. 7. The spectra change very smoothly with the regularization parameter $q$, when the latter varies by an order of magnitude. A small $q$ gives highly resolved multiplets but also retains some small spikes. When $q$ is increased the spectrum becomes more uniform and smooth decreasing the resolution. With large values

of $q$ the multiplet structure is unresolved and some, generally weak, peaks disappear in the contour plot as they are effectively broadened by the regularization. Note that the spectrum corresponding to $q = 0.01$ is much better resolved than that in ref. [7] where a "naive" 2D FDM was used. Also note that in ref. [7] the signal was much shorter in the running time dimension to simplify the frequency identification procedure, which is completely avoided here due to the use of the resolvent formulae.

## 5. Conclusions and Future work

Both 1D FDM and RRT (that emerged from FDM) are essentially developed and well tested techniques that are generally as reliable as FFT, sufficiently fast, and can often deliver resolution beyond the FT uncertainty relation if the data can be well represented by Lorentzians and is not very noisy. FDM provides one with an effective evolution operator $\hat{U}$ whose eigenvalues and eigenvectors are directly related to the spectral parameters. However, the difficulties associated with the construction of a meaningful line list for data of poor quality (i.e., not characterized by Eq. 3) exist. These difficulties are not associated with the lack of a reliable algorithm of selecting the "genuine" poles and throwing away the "noise" poles from the full list of complex eigenvalues of $\hat{\Omega}$ , but are rather conceptual caused by the ambiguity of the line list for a general data that, *a priori*, does not fit any particular parametric form.

The multidimensional spectrum cannot be generally constructed from the multidimensional line list as the latter is very hard to obtain. Fortunately, various spectra can be obtained by avoiding the line list construction and using the resolvent expressions. The resolvent operator formalism appears to be very convenient since it allows to construct various types of spectra including absorption-mode spectra, non-trivial spectral projections. The main computational problem associated with the implementation of the resolvent formulae is that one typically deals with very ill-conditioned matrices causing the spectrum to be very unstable with respect to both the FDM parameters and small variations of the input data. Thus, unlike the 1D case, there are major problems to be solved in the multidimensional

versions of both FDM and RRT. Clearly, the key issue of D> 1 FDM is to find a general computationally inexpensive and robust procedure that could be applied to regularize the FDM equations. At the present stage the problem is solved only partially.

To conclude, the main avenues for the future research seem to be the following.

(i) Given the matrix representations of the evolution operators $\hat{U}^{(p)}$ in a non-orthonormal basis, find a fast and reliable method of evaluating various resolvents associated with these operators.

(ii) Given the matrix representations of the evolution operators, construct a set of commuting effective Hamiltonians $\hat{\Omega}_1$,$\hat{\Omega}_2$, etc., whose eigenvalues and eigenvectors yield the line list.

Both goals are associated with finding a reliable and computationally inexpensive regularization.

## 6. ACKNOWLEDGEMENTS

Vladimir A. Mandelshtam and A. J. Shaka

Department of Chemistry, University of California, Irvine

## References

[1] J. C. Hoch, A. S. Stern *NMR Data Processing* (1996)

[2] D. Neuhauser, *J. Chem. Phys.* **93**, 2611-2616 (1990).

[3] M. R. Wall and D. Neuhauser, *J. Chem. Phys.* **102**, 8011-8022 (1995).

[4] V. A. Mandelshtam, and H. S. Taylor, *J. Chem. Phys.* **107**, 6756-6769 (1997).

[5] V. A. Mandelshtam, and H. S. Taylor, *J. Chem. Phys.* **108**, 9970-9977 (1998).

[6] V. A. Mandelshtam, H. S. Taylor, and A.J. Shaka, *J. Magn. Reson.* **133**, 304-312 (1998).

[7] V. A. Mandelshtam, H. Hu and A.J. Shaka, *Magn. Res. Chem.* **36**, S17-S28 (1998).

[8] H. Hu, Q.N. Van, V. A. Mandelshtam and A.J. Shaka, *J. Magn. Reson.* **134**, 76-87 (1998).

[9] J.W. Pang, T. Dieckmann, J. Feigon, D. Neuhauser, *J. Chem. Phys.* **108**, 8360-8368 (1998).

[10] M.R. Wall, T. Dieckmann, J. Feigon, D. Neuhauser, *Chem. Phys. Lett.* **291**, 465-470 (1998).

[11] V. A. Mandelshtam, Q.N. Van and A.J. Shaka, *J. Am. Chem. Soc.* **120**, 12161 (1998).

[12] V. A. Mandelshtam, N.D. Taylor, H. Hu, M. Smith, and A.J. Shaka, *Chem. Phys. Lett.* **305**, 209 (1999).

[13] J. Chen and V. A. Mandelshtam, *J. Chem. Phys.* **112**, 4429 (2000)

[14] V. A. Mandelshtam, *J. Magn. Reson.* **144**, 343 (2000).

[15] H. Hu, A. A. De Angelis, V. A. Mandelshtam, A. J. Shaka *J. Magn. Reson.* **144**, 357 (2000)

[16] V. A. Mandelshtam, and H. S. Taylor, *Phys. Rev. Lett.* **78**, 3274-3277 (1997).

[17] W. H. Press, S. A. Teukolsky, W. T. Vetterling, and B. P. Flannery, *Numerical Recipe in C*, 2nd Edition (1992)

[18] B. F. Volkman, A. M. Prantner, S. J. Wilkens, B. Xia, and J. L. Markley, *J. Biomol. NMR* **10** 409 (1997)

[19] J. Chen, A. J. Shaka and V. A. Mandelshtam *J. Magn. Reson.* (submitted)

[20] J. Chen, V. A. Mandelshtam and A. J. Shaka *J. Magn. Reson.* (submitted)

[21] A. Tikhonov, Solution of incorrectly formulated problems and the regularization method, *Soviet Math. Dokl.* **4**, 1035-1038 (1963); A. Tikhonov and V. Arsenin, Solutions of ill-posed problems. Winston and Sons, Washington (1977).

[22] V. A. Mandelshtam, *J. Magn. Reson.* (submitted)

[23] J. Chen, A. J. Shaka and V. A. Mandelshtam, unpublished results.

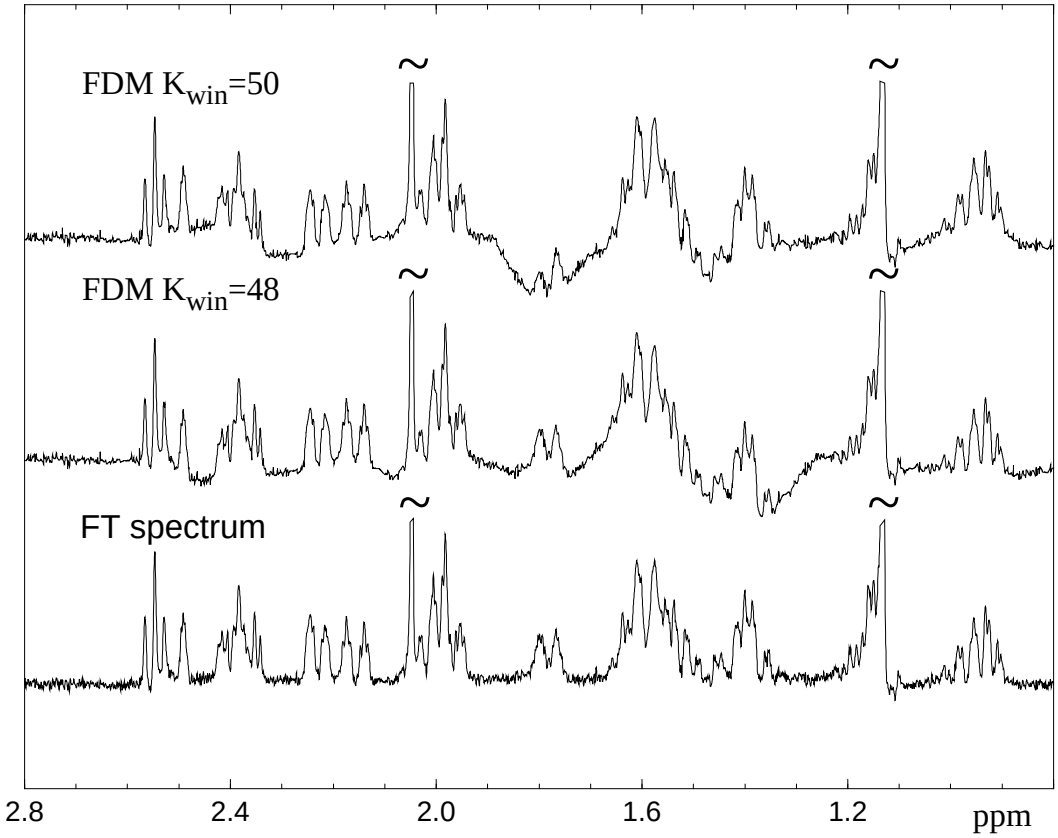


FIG. 1. Spectra obtained from a noisy 1D NMR signal of length $N = 2000$ and spectral width $SW = 4$ ppm (2kHz) using two different methods, FT with an appropriate apodization (bottom) and FDM (the upper two traces). The FDM ersatz spectra used slightly different numbers, $K_{\rm win} = 48$ and $K_{\rm win} = 50$, of the Fourier basis functions per window, corresponding to bandwidths 0.192 ppm and 0.2 ppm, respectively. Note that a multi-window approach (see text) was used to construct the overall FDM spectra.

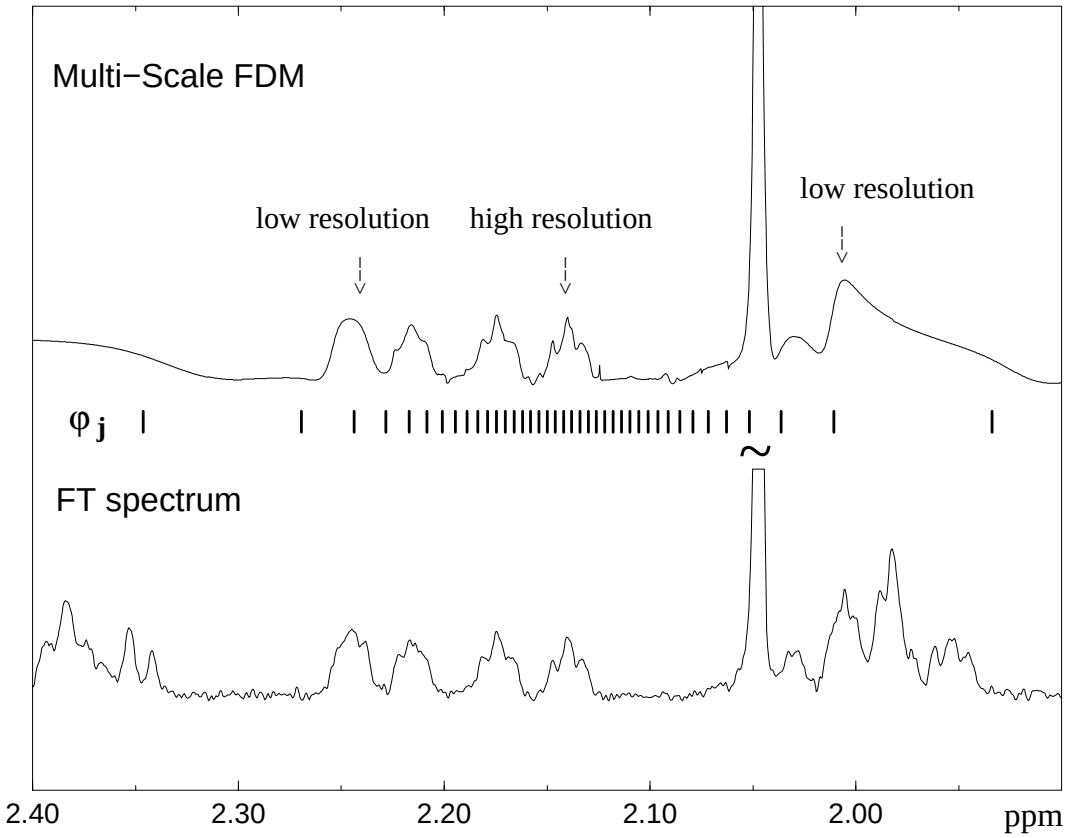


FIG. 2. An example of a multi-scale basis set and the spectrum obtained using this basis for the same signal used in Fig. 1. $K_{\rm win} = 10$ narrow band and $K_c = 20$ coarse basis functions (indicated by an impulse at each $\varphi_j$) were used. The coarse functions are distributed non-uniformly according to the displacement from the window (see text).

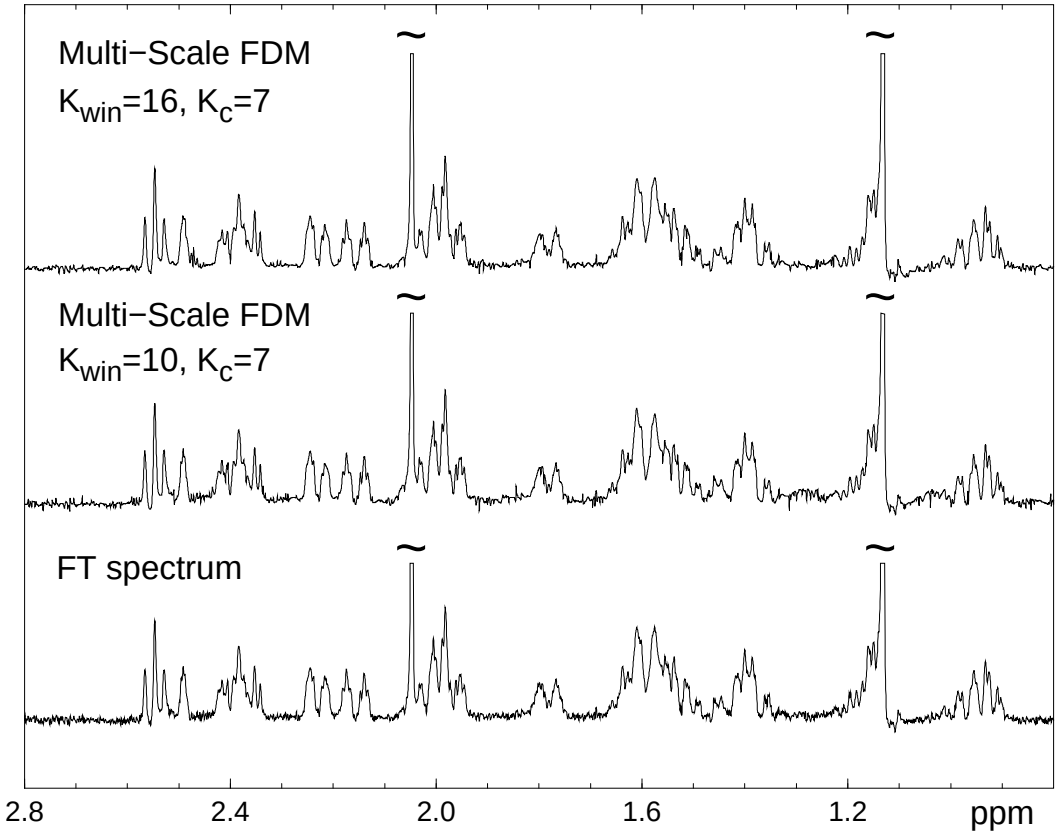


FIG. 3. A comparison of FT and multi-scale FDM ersatz spectra generated by Eq. 4. The overall basis as small as $K_{\rm win} + K_c = 10 + 7 = 17$ still gives a reasonable spectrum. Further increase of the window basis to $K_{\rm win} = 16$ leads to an absolutely converged result in that it is stable and insensitive to the FDM parameters used, such as basis size, window position etc.

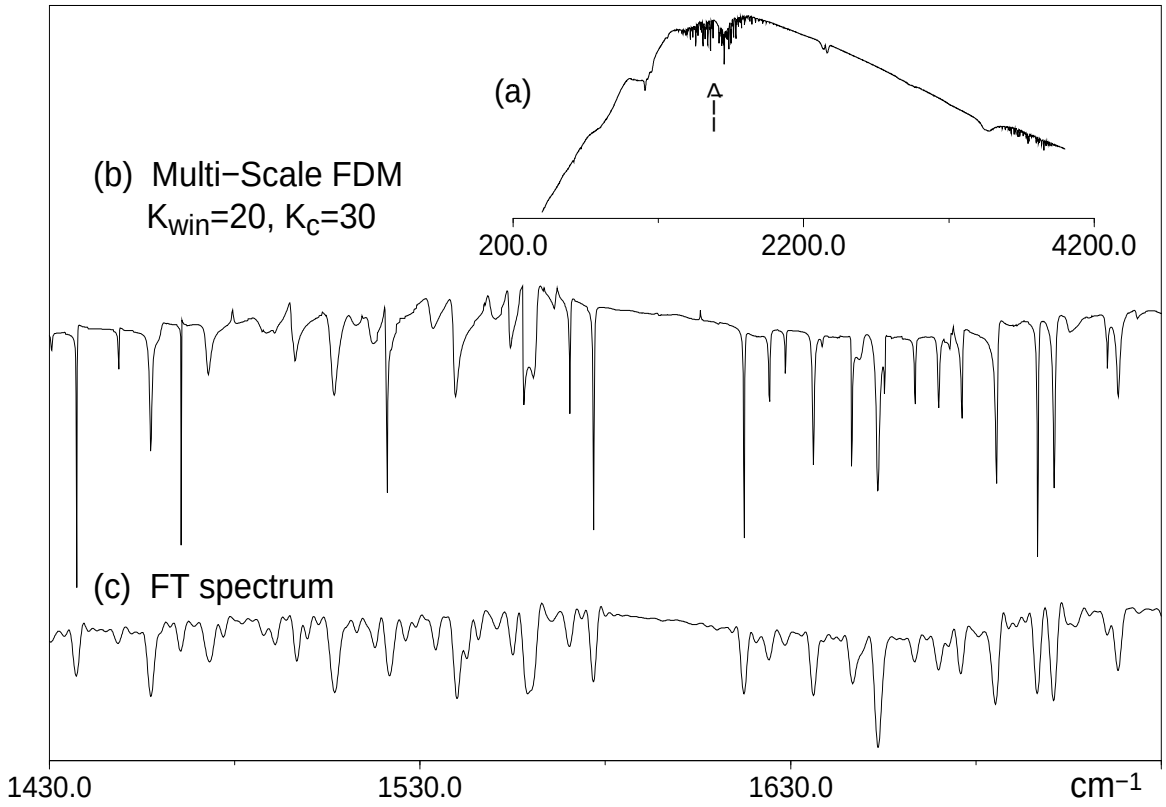


FIG. 4. FT-IR spectrum (a) and an interesting part of the same spectrum processed by the multi-scale FDM with $K_{\rm win} + K_c = 20 + 30 = 50$ (b) and by FT (c). The interferogram contained 4744 data points.

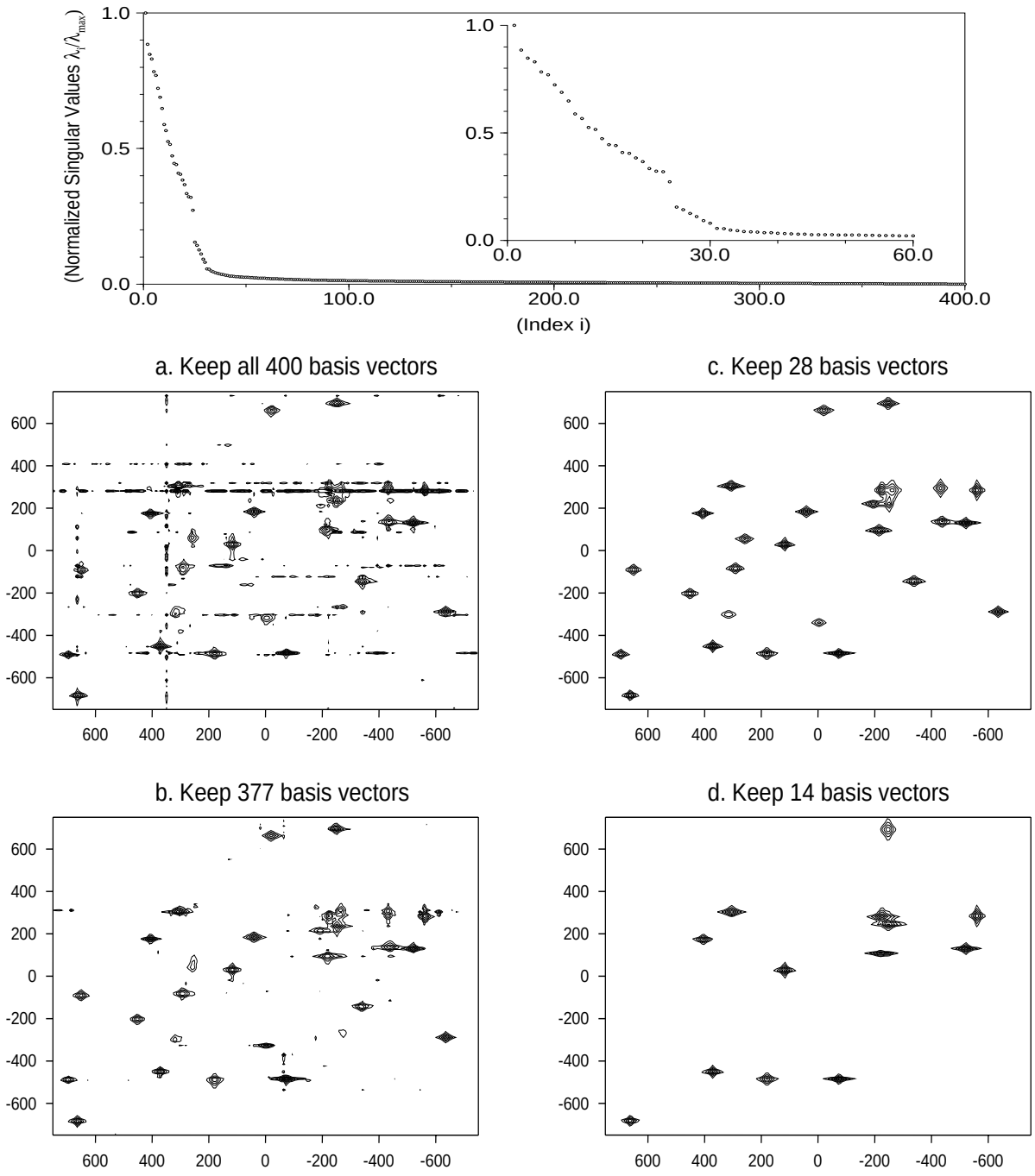


FIG. 5. Chemical shift correlation spectra obtained by FDM using SVD to reduce the basis size (see text). The signal length processed is $N_1 \times N_2 = 200 \times 8$ and total basis size is $Nb_{\text{total}} = 50 \times 8 = 400$. The top panel shows the distribution of singular values of overlapping matrix $\mathbf{U}_0$. The four spectra below (a,b,c,d) are obtained by diagonalizing the $\mathbf{U}$ matrices in different size of reduced basis provided by SVD of $\mathbf{U}_0$.

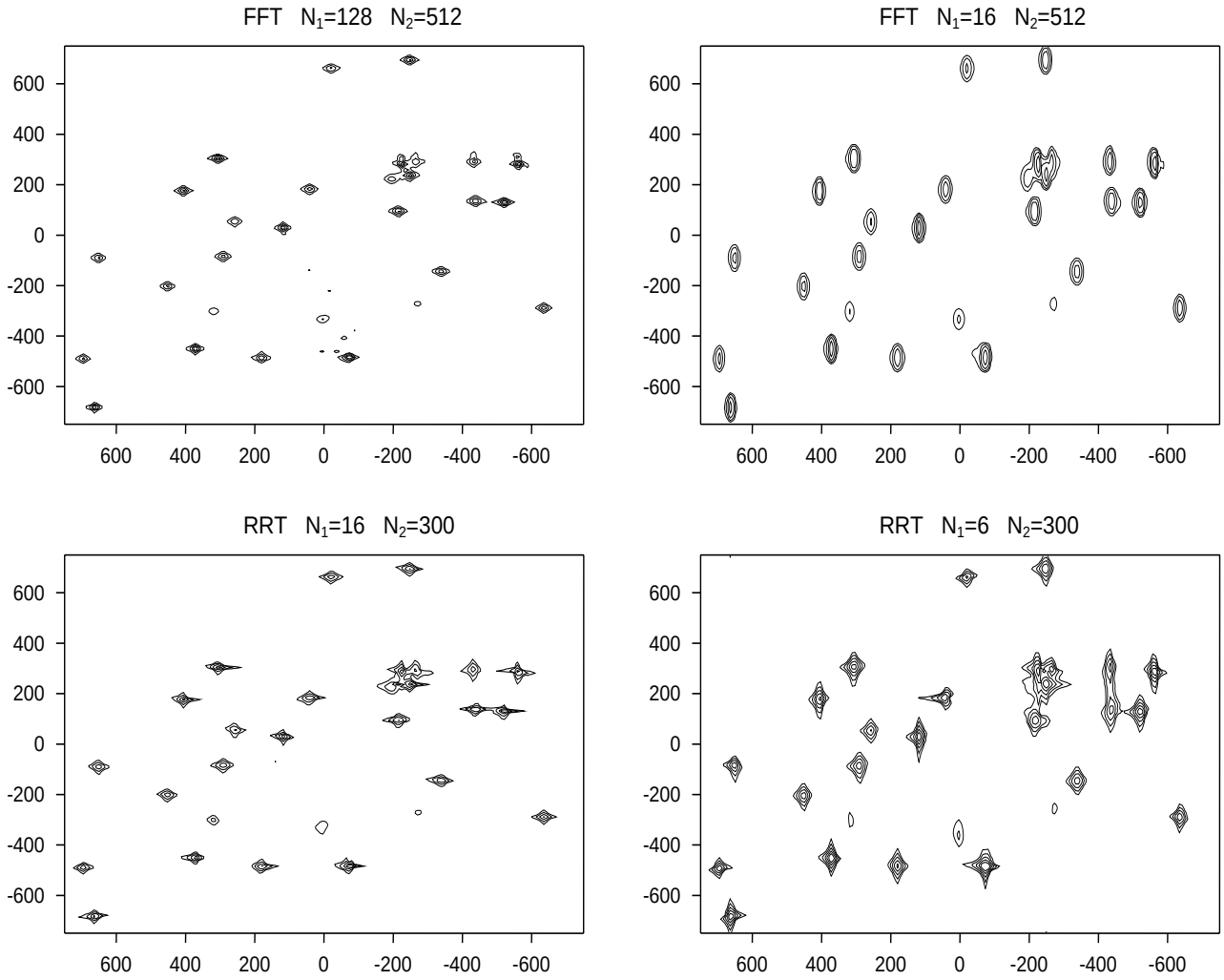


FIG. 6. Chemical shift correlation spectra of the metalloprotein rubredoxin obtained with gradient selection of the coherence transfer pathway and processed by Regularized Resolvent Transfrom (RRT) and discrete Fourier Transform (DFT). Each of the double-absorption spectra were generated using the conventional procedure that combines the complex N- and P-type spectra.

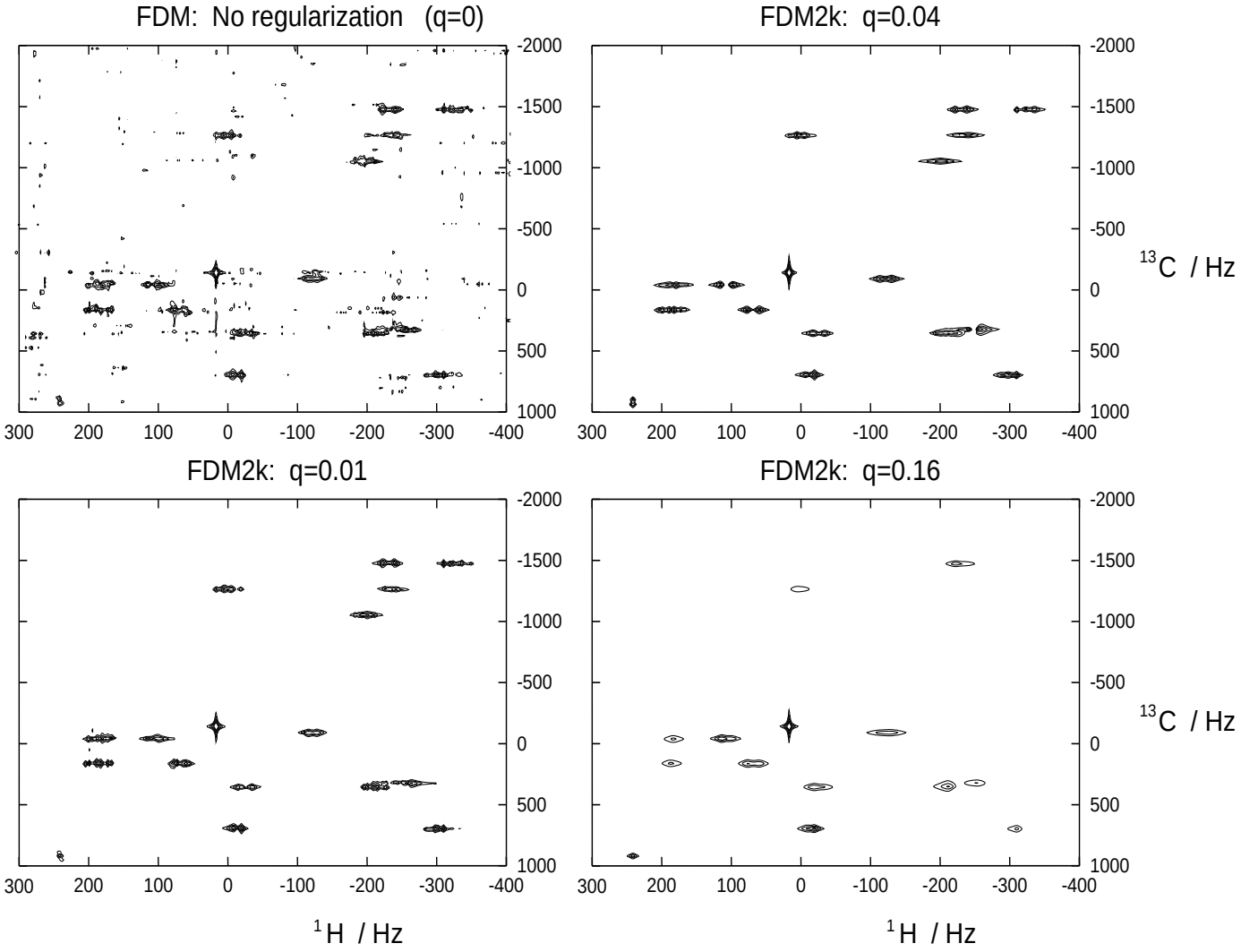


FIG. 7. A non-regularized ($q = 0$) and regularized ($q > 0$) spectra using FDM2K (see Eq. 45) applied to a purely phase modulated 2D signal, generated by an HSQC pulse sequence applied to progesterone (see text and Refs. [7,15] for more detail). The data set processed consisted of $N_1 \times N_2 = 600 \times 64$ in the proton and the carbon-13 dimensions, respectively. Only a small crowded region of the spectrum is shown, the spectral widths being $SW_1 = 2000$ Hz and $SW_2 = 8625$ Hz. The spectra were generated by combining the results of 8 small overlapping windows, each described by $K_{\rm win} = K_{1\rm win} \times K_{2\rm win} = 24 \times 12 = 288$ Fourier basis functions.